



Citation for published version:

Hussain, A, Calabria-Holley, J, Schorr, D, Jiang, Y, Lawrence, M & Blanchet, P 2018, 'Hydrophobicity of Hemp Shiv treated with Sol-gel Coatings', *Applied Surface Science*, vol. 434, pp. 850-860.
<https://doi.org/10.1016/j.apsusc.2017.10.210>

DOI:

[10.1016/j.apsusc.2017.10.210](https://doi.org/10.1016/j.apsusc.2017.10.210)

Publication date:

2018

Document Version

Peer reviewed version

[Link to publication](#)

Publisher Rights

CC BY-NC-ND

University of Bath

Alternative formats

If you require this document in an alternative format, please contact:
openaccess@bath.ac.uk

General rights

Copyright and moral rights for the publications made accessible in the public portal are retained by the authors and/or other copyright owners and it is a condition of accessing publications that users recognise and abide by the legal requirements associated with these rights.

Take down policy

If you believe that this document breaches copyright please contact us providing details, and we will remove access to the work immediately and investigate your claim.

2

3 **Hydrophobicity of Hemp Shiv treated with Sol-gel Coatings**

4

5 **Atif Hussain^{a, b,*}, Juliana Calabria-Holley^a, Diane Schorr^b, Yunhong Jiang^a, Mike Lawrence^a,**
6 **Pierre Blanchet^b**

7 ^aBRE Centre for Innovative Construction Materials, Department of Architecture and Civil
8 Engineering, University of Bath, Bath BA2 7AY, UK

9 ^bNSERC Industrial Research Chair on Ecoresponsible Wood Construction, Department of Wood
10 and Forest Sciences, Université Laval, Quebec, QC, G1V 0A6, Canada

11 *Corresponding Author: Atif Hussain (A.Hussain@bath.ac.uk)

12

13 **Abstract**

14 This is the first time sol-gel technology is used in the treatment of hemp shiv to develop
15 sustainable thermal insulation building materials. The impact on the hydrophobicity of hemp shiv
16 by depositing functionalised sol-gel coatings using hexadecyltrimethoxysilane (HDTMS) has been
17 investigated. Bio-based materials have tendency to absorb large amounts of water due to their
18 hydrophilic nature and highly porous structure. In this work, the influence of catalysts, solvent
19 dilution and HDTMS loading in the silica sols on the hydrophobicity of hemp shiv surface has been
20 reported. The hydrophobicity of sol-gel coated hemp shiv increased significantly when using acid
21 catalysed sols which provided water contact angles of up to 118° at 1% HDTMS loading. Ethanol
22 diluted sol-gel coatings enhanced the surface roughness of the hemp shiv by 36% as observed
23 under 3D optical profilometer. The XPS results revealed that the surface chemical composition of
24 the hemp shiv was altered by the sol-gel coating, blocking the hydroxyl sites responsible for
25 hydrophilicity.

26

27 **Keywords**

28 Sol-gel, hydrophobicity, coatings, surface roughness, hemp shiv

29

30

31 1. Introduction

32 Wettability of a solid surface is governed by a combination of chemical composition and geometric
33 structure of the surface [1,2]. The interplay between surface chemistry and surface roughness
34 has been an active research topic for enhancing the hydrophobicity of cellulose based materials.

35
36 The woody core of the hemp plant (*Cannabis Sativa* L.) known as shiv has gained interest in the
37 building industry during the recent years for production of lightweight composites. Hemp shiv
38 based composites have interesting properties such as thermal [3], hygroscopic [4], mechanical,
39 acoustic [5] and biodegradability [6].

40
41 Hemp shiv are generally very porous with low density tending to absorb large amounts of water.
42 Previous studies have reported that hemp shiv not only has higher water absorption rate but also
43 absorb high amounts of water in the very first minutes compared to different plant materials [7].
44 Moreover, the presence of cellulose, hemicellulose and lignin in bio-based materials contributes
45 to the presence of hydroxyl groups in their structure. This leads to certain disadvantages of using
46 bio-based materials making them incompatible with hydrophobic thermoset/thermoplastic
47 polymers [8]. High moisture uptake also encourages colonial fungal growth resulting in cell wall
48 degradation and lower durability of the material [9].

49
50 The major constituents of industrial hemp shiv are: cellulose (44%), hemicellulose (18-27%), lignin
51 (22-28%) and other components such as extractives (1-6%) and ash (1-2%) [10,11]. Cellulose is
52 a semi crystalline polysaccharide consisting of linear chain of several D-glucose units linked
53 together by β (1–4) glucosidal bond. Cellulose contains free hydroxyl groups, and since they form
54 the major structural component of hemp shiv, they are responsible for the extreme hydrophilic
55 behaviour.

56
57 One of the mechanism to convert cellulose–based material from hydrophilic to hydrophobic
58 involves chemical modification to block the hydroxyl groups of the cell wall thereby reducing water
59 sorption sites. Treatments include acetylation [12], silanization [13] and in situ polymerization [14]
60 that involve incorporation of materials into the cell wall blocking the voids accessible to water
61 molecules. Other treatments methods that are known to enhance the water repellence are plasma
62 etching, lithography, electrospinning and sol-gel treatment that endow the material with nano-
63 scale surface roughness [15].

64
65 Chemical pre-treatment of natural plant materials have reported better bonding with polymer
66 matrix interface due to improvement of their hydrophobic characteristics [16]. There is a need to
67 develop a novel treatment method for hemp shiv to enhance its water resistance thereby
68 improving the shiv-binder interfacial adhesion and reduce its susceptibility to decay. The sol-gel
69 technique is a highly versatile method to deposit silica based coatings possessing single or multi
70 functionality [17]. These thin mesoporous coatings have high structural homogeneity and their
71 adhesion can be tailored to different substrates.

72
73 Sol-gel based hydrophobic and water repellent coatings have been investigated on different bio-
74 based materials such as wood [18] and cellulosic fibres [19], however for hemp shiv this is the
75 first time. The reactive hydroxyl groups present in the polysiloxane network of the sol-gel combine
76 with the hydroxyl groups of cellulose through a covalent bond. This study successfully delivers a
77 sol-gel modified hemp shiv material of hydrophobic character through a simple and inexpensive,
78 one step dip-coating method.

79

80 **2. Experimental**

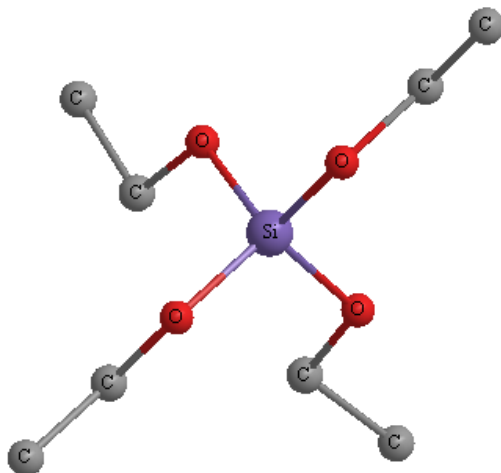
81

82 **2.1 Materials**

83 Hemp shiv used in this study was received from MEM Inc., manufacturer of ecological materials
84 based in Rimouski, Canada. Tetraethyl orthosilicate (TEOS, 98%) and hexadecyltrimethoxysilane
85 (HDTMS, 85%) were obtained from Sigma-Aldrich. Anhydrous ethanol was purchased from
86 Commercial Alcohols, Canada. Hydrochloric acid (HCl, 38%) and nitric acid (HNO₃, 70%) were
87 obtained from Anachemia, VWR, Canada. All chemicals were used as received without further
88 purification.

89

(A)



90

(B)

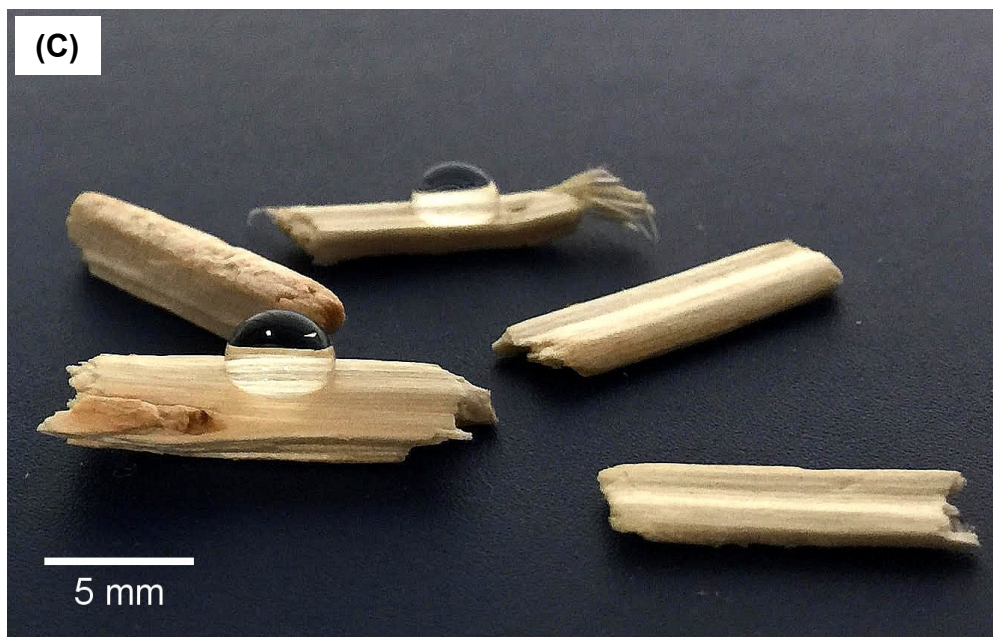


91

92

93

(C)



94

95

Figure 1. 3D structure of a (A) TEOS molecule, (B) HDTMS molecule; and (C) water on coated hemp shiv samples.

96

97 It is known that HDTMS may not be able to penetrate the outer surface layers of the cell wall due
98 to its high molecular weight [18]. Due to this, the hydrophobicity would be compromised and it can
99 be predicted that the coating might not be robust. Moreover, using only HDTMS would be highly
100 expensive and would not be of interest to the construction industry. For these reasons, it was
101 considered inappropriate to make a comparative study using purely HDTMS.

102

103

104 **2.2 Preparation of the hydrophobic coatings**

105 The silica based sol-gel was synthesised by hydrolysis and condensation of TEOS in ethanol and
106 water. The reaction was catalysed using 0.005M acid (HCl/ HNO₃). Two sets of silica sols were
107 prepared based on the difference in concentration of ethanol. The first set of formulations (sols
108 A) were prepared stirring 1M TEOS in a mixture of 4M water and 4M ethanol. For the preparation
109 of the second set of formulations (sols B), 1M TEOS was added to 4M water and 16M ethanol.
110 After the preparation of both sets of silica formulations, the hydrophobic agent HDTMS was added
111 in concentrations of 0.5-4 wt% of the sol. These mixtures of silica sol and HDTMS were stirred at
112 300 rpm for at least 20 minutes before performing the dip-coating process. All the sols were
113 prepared at 40 °C and atmospheric pressure. The sols were allowed to cool down to room
114 temperature and the pH was recorded.

115

116 The sols aged for 48 hours in closed container at room temperature before the dip-coating
117 process. Gelation took place in-situ in which pieces of hemp shiv were dipped in the sol for 10
118 min and then carefully removed and transferred onto a Petri dish. The samples were placed at
119 room temperature for one hour and then dried at 80 °C for one hour. A schematic illustration of
120 the HDTMS modified silica sol-gel coating is shown in Figure 1.

121

122 As for the preparation of the pure sol-gel specimen, the sol aged in a container at room
123 temperature until gel point. The gel-point was taken as the time when the sol did not show any
124 movement on turning the container upside down. The gel-time and pH for all the prepared sols
125 are reported in Table 1.

126

127 *Table 1. Composition of the prepared sol-gel formulations and their properties.*

FORMULATION	CATALYST	ETHANOL CONC. (M)	HDTMS CONC. (wt%)	GEL TIME (DAYS)	pH
sol A-1	HCl	4.0	4.0	178	1.87
sol A-2	HCl	4.0	2.0	116	1.82
sol A-3	HCl	4.0	1.0	101	1.78
sol A-4	HCl	4.0	0.5	101	1.85
sol A-5	HNO ₃	4.0	4.0	150	1.73
sol A-6	HNO ₃	4.0	2.0	112	1.87
sol A-7	HNO ₃	4.0	1.0	101	1.92
sol A-8	HNO ₃	4.0	0.5	101	1.92
sol B-1	HCl	16.0	4.0	>180	1.64
sol B-2	HCl	16.0	2.0	>180	1.68
sol B-3	HCl	16.0	1.0	>180	1.67
sol B-4	HCl	16.0	0.5	>180	1.72
sol B-5	HNO ₃	16.0	4.0	>180	1.70
sol B-6	HNO ₃	16.0	2.0	>180	1.76
sol B-7	HNO ₃	16.0	1.0	>180	1.81
sol B-8	HNO ₃	16.0	0.5	>180	1.83

128

129 **2.3 Contact Angle Measurements**

130 The water contact angle (WCA) of uncoated and coated hemp shiv samples were measured using
 131 a contact angle meter (First Ten Ångströms USA, FTA200 series). The sessile drop method was
 132 employed and the contact angle was determined on at least three different positions for each
 133 sample (coated substrate). **The volume of the water droplets was 5µl for the contact angle**
 134 **measurements.** The average value was adopted as a final value. Images were captured and
 135 analysed using the FTA32 Video 2.0 software. All the measurements were performed at room
 136 temperature (24 ± 1 °C).

137

138 **2.4 Surface Roughness**

139 The topography and surface roughness of the samples was obtained using a 3D optical
140 profilometer (Bruker Nano GmbH Germany, ContourGT-K series). The surface roughness was
141 measured over an area at 0.25*0.30 mm² in non-contact mode at 20X magnification. Vision 64
142 on board software was then employed to analyse these data and calculate the roughness
143 parameters. The readings were taken on at least three different positions for each sample and
144 the average value was reported as the final value.

145

146 **2.5 X-ray photoelectron spectroscopy (XPS)**

147 The surface elemental and chemical composition of the samples were analysed using XPS. Prior
148 to XPS analysis, samples were oven-dried at 80 °C for 96 hours. XPS spectra of uncoated and
149 sol-gel coated hemp shiv were recorded with an X-ray photoelectron spectrometer (Kratos Axis
150 Ultra, UK). All spectra were collected using a monochromatic Al K α X-ray source operated at 300
151 watts. The lateral dimensions of the samples were 800 microns \times 400 microns, corresponding to
152 those of the Al K α X-ray used, and probing depth was approximately 5 nanometres. For each
153 sample, two spectra were recorded: (i) survey spectra (0–1150 eV, pass energy 160 eV, and step
154 size 1eV) recorded for apparent composition calculation; and (ii) high-resolution C1s, O1s and Si
155 2p spectra (within 20 eV, pass energy 20 eV and step size within 0.05eV) recorded to obtain
156 information on chemical bonds. Calculation of the apparent relative atomic concentrations is
157 performed with the CasaXPS software. Peak fitting is performed with CasaXPS, which
158 automatically and iteratively minimizes the difference between the experimental spectrum and the
159 calculated envelope by varying the parameters supplied in a first guess.

160

161 **2.6 Scanning Electron Microscopy**

162 The surface morphology of the specimens was characterised using a scanning electron
163 microscopy (SEM), JEOL corporation - Japan Model JSM-6360 operating at 25 kV. The
164 specimens were coated with gold to achieve maximum magnification of textural and
165 morphological characteristics.

166

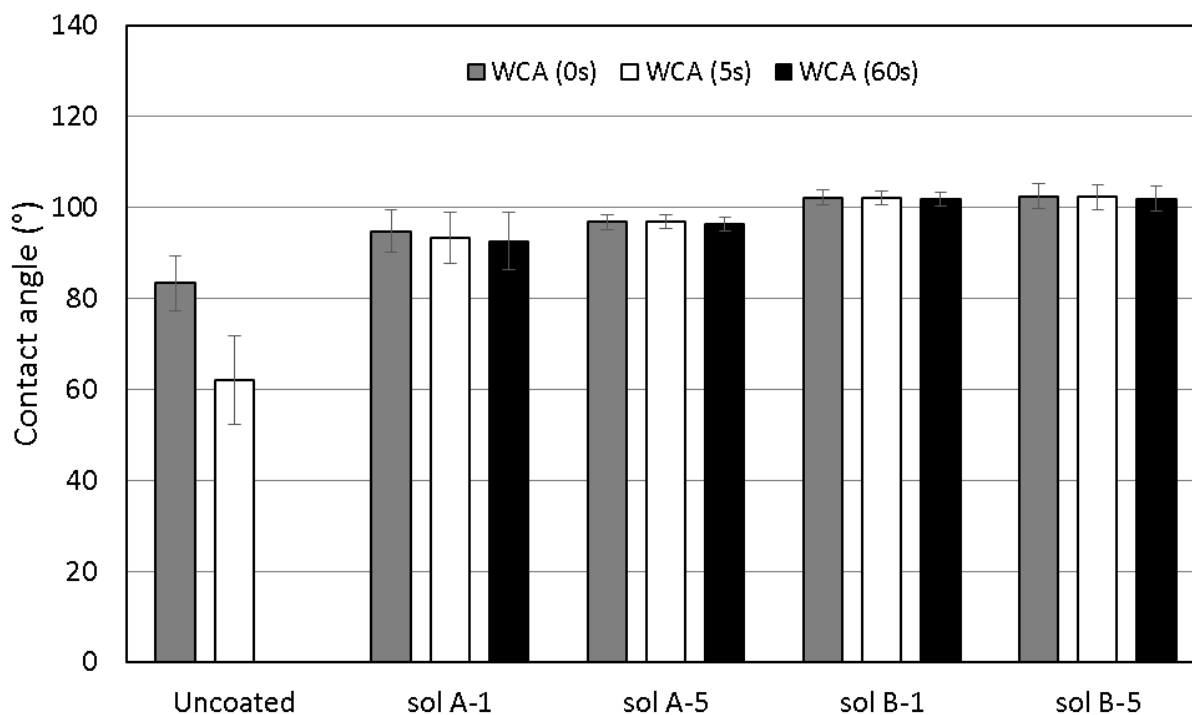
167

3. Results

3.1 Hydrophobicity of sol-gel coatings

169 The water contact angle was determined as soon as the water droplet encountered the sol-gel
170 coated hemp shiv surface. The sol-gel coatings with high HDTMS loadings (4 wt%) and varying
171 concentration of ethanol are compared in Figure 2. It can be seen that uncoated shiv has an
172 extremely hydrophilic surface and water droplet sinks into the substrate reducing the WCA in a
173 short time. The sol-gel coatings yield hydrophobicity to the hemp shiv by maintaining a stable
174 contact angle over 60 seconds.

175



176

177 *Figure 2. Hydrophobicity of hemp shiv surface treated with different sol-gel coatings over 60 seconds of water contact.*

178

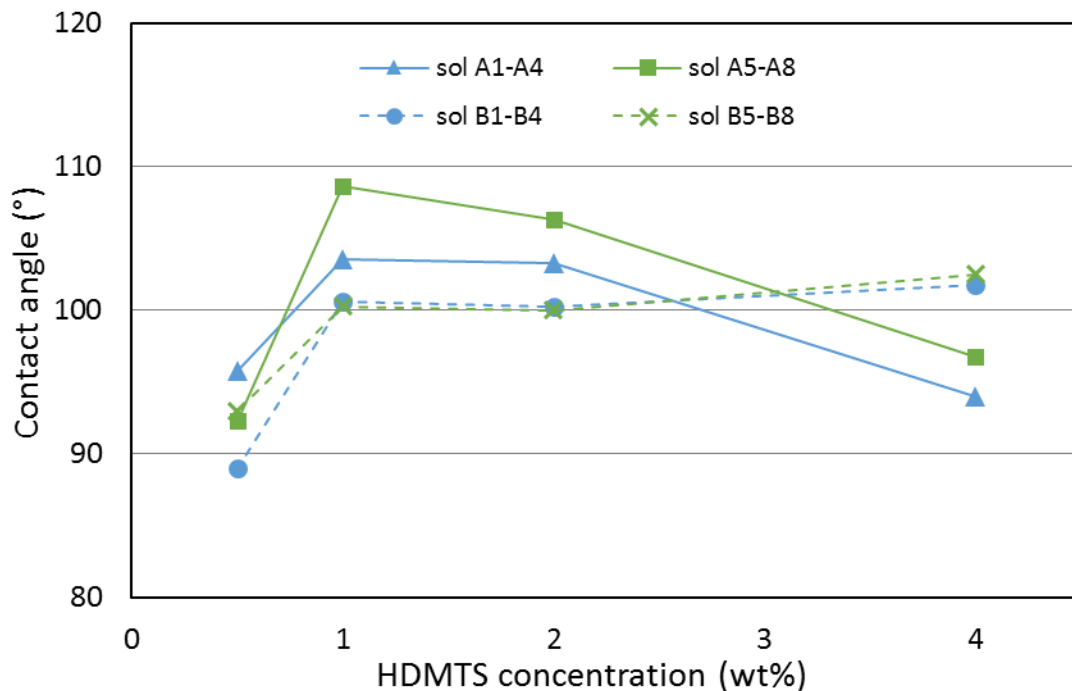
179 Considering the coating compositions with 4% HDTMS loading listed in Table 1, it was observed
180 that ethanol diluted sols (sol B series) performed better in terms of providing hydrophobicity to
181 hemp shiv surface compared to undiluted sols (sol A series). Sol B-1 and sol B-5 coatings had
182 higher contact angles (up to 105°) compared to sol A-1 and sol A-5 coatings (up to 100°).

183

184 Ethanol helps the HDTMS to be fully dissolved in water thereby promoting the hydrolysis
185 reaction [20,21]. Figure 2 shows the WCA measurements of sol coatings containing 4 wt%
186 HDTMS. Sol A-1 and sol A-5 contain only 4M ethanol whereas sol B-1 and sol B-5 contain
187 16M of ethanol. At 4 wt% HDTMS concentration, using 16M of ethanol favours the hydrolysis
188 of HDTMS. In this way HDTMS molecules are able to self-assemble on the silica network,
189 hence providing enhanced hydrophobicity to the material. In general, it was observed that sol-
190 gel coatings with HNO₃ as catalyst perform slightly better in terms of hydrophobicity than coatings
191 with HCl as catalyst.

192

193 The changes in water contact angle as a function of HDTMS loading (0.5-4.0 wt%) is presented
194 in Figure 3. The contact angle measurements had a standard deviation between 1.1° and 6.0°.
195 The hydrophobic performance of the coatings is not reduced on lowering the HDTMS loading
196 down to 1%. Surfaces coated with sol B series showed good water repellence with contact angles
197 ranging between 96° to 108°.



198

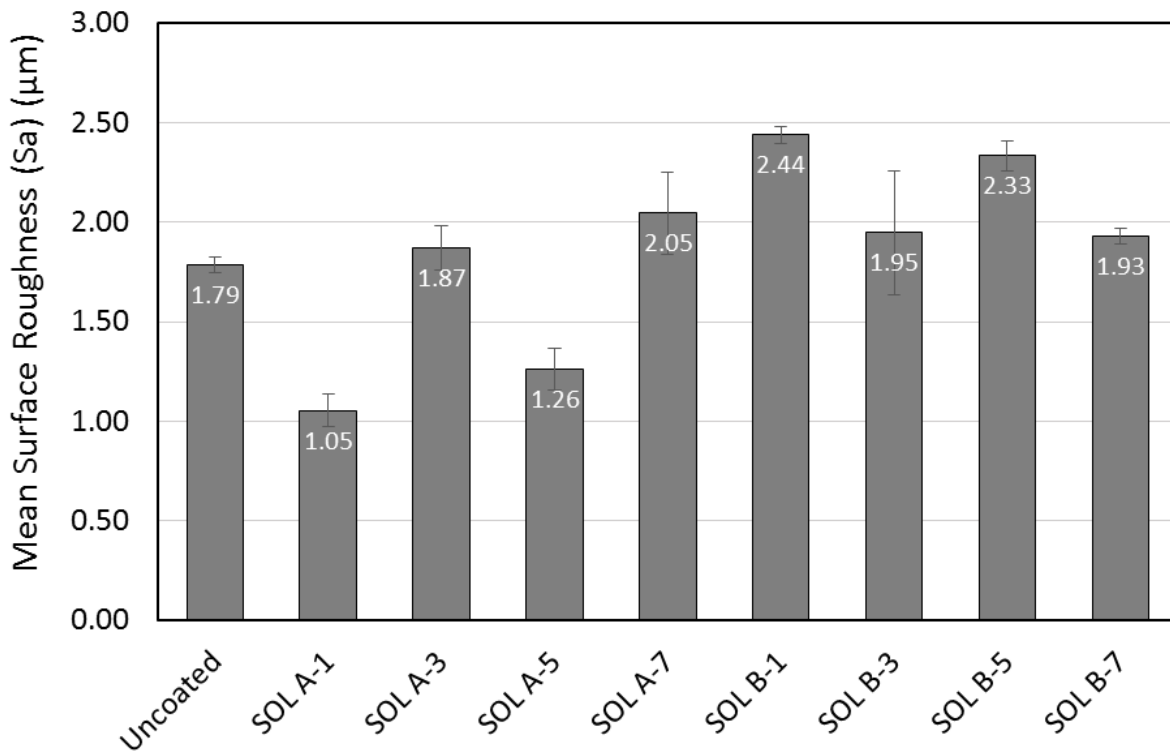
199 *Figure 3. Effect of ethanol dilution and varying HDTMS concentration in the sol-gel coating on hydrophobicity of hemp*
200 *shiv surface.*

201

202 **3.2 Surface roughness of the coatings**

203 The samples were analysed for their surface microstructure and roughness by the Vision64
204 software using a Robust Gaussian Filter (ISO 16610-31 2016) and a short wavelength cut-off
205 0.025mm. The use of such filters helps to reduce the anatomical influence and optimizes the
206 roughness profile data for evaluation of the sample surface [22,23]. The robust Gaussian filter
207 avoids the distortions produced by some filters when applied in profiles with deep valleys [24].
208 Mean surface roughness (S_a) was calculated according to ISO 4287 (1997). S_a gives the
209 description of the height variations in the surface and it is the most widely used parameter to
210 measure the surface roughness profile of the sample. The surface roughness parameters for sol-
211 gel coated hemp shiv with 1% and 4% HDTMS loadings are shown in Figure 4.

212



213

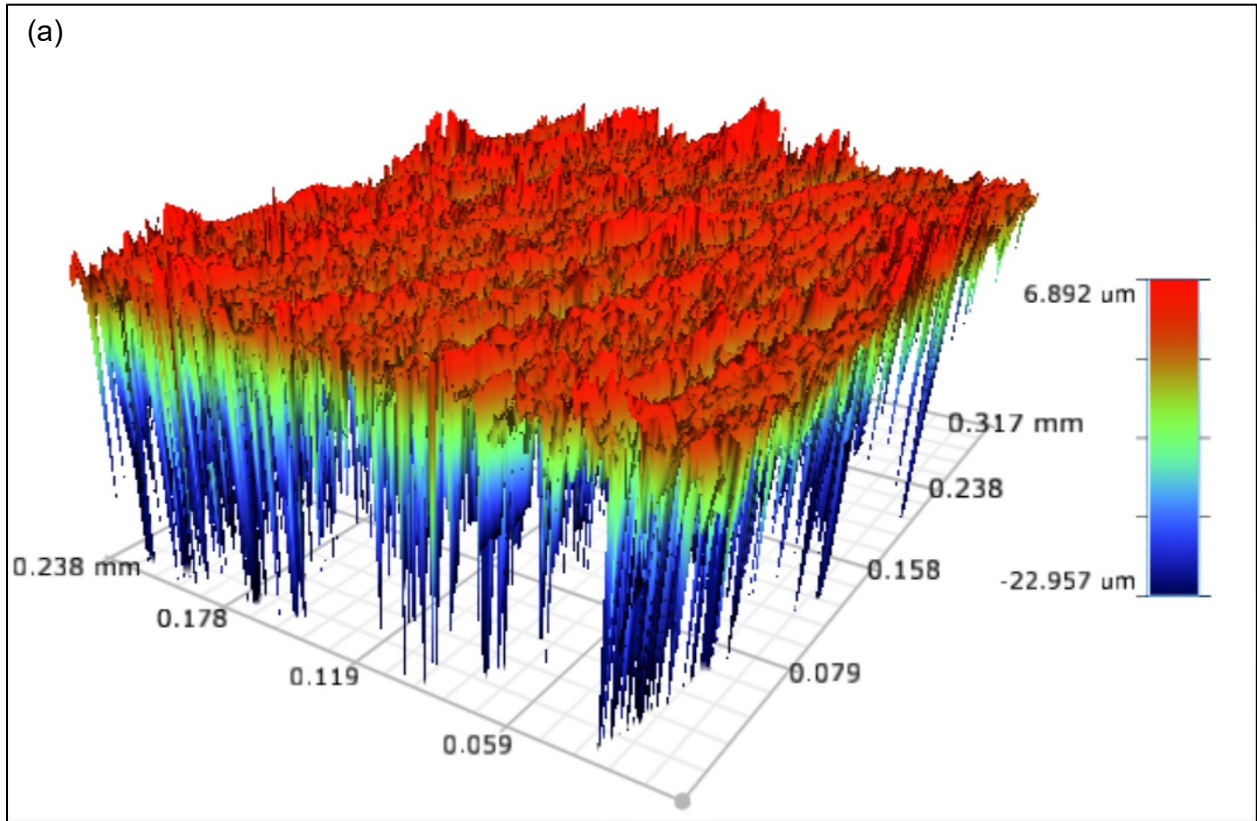
214 *Figure 4. Mean surface roughness (S_a) measurement of uncoated and sol-gel coated hemp shiv surfaces.*

215

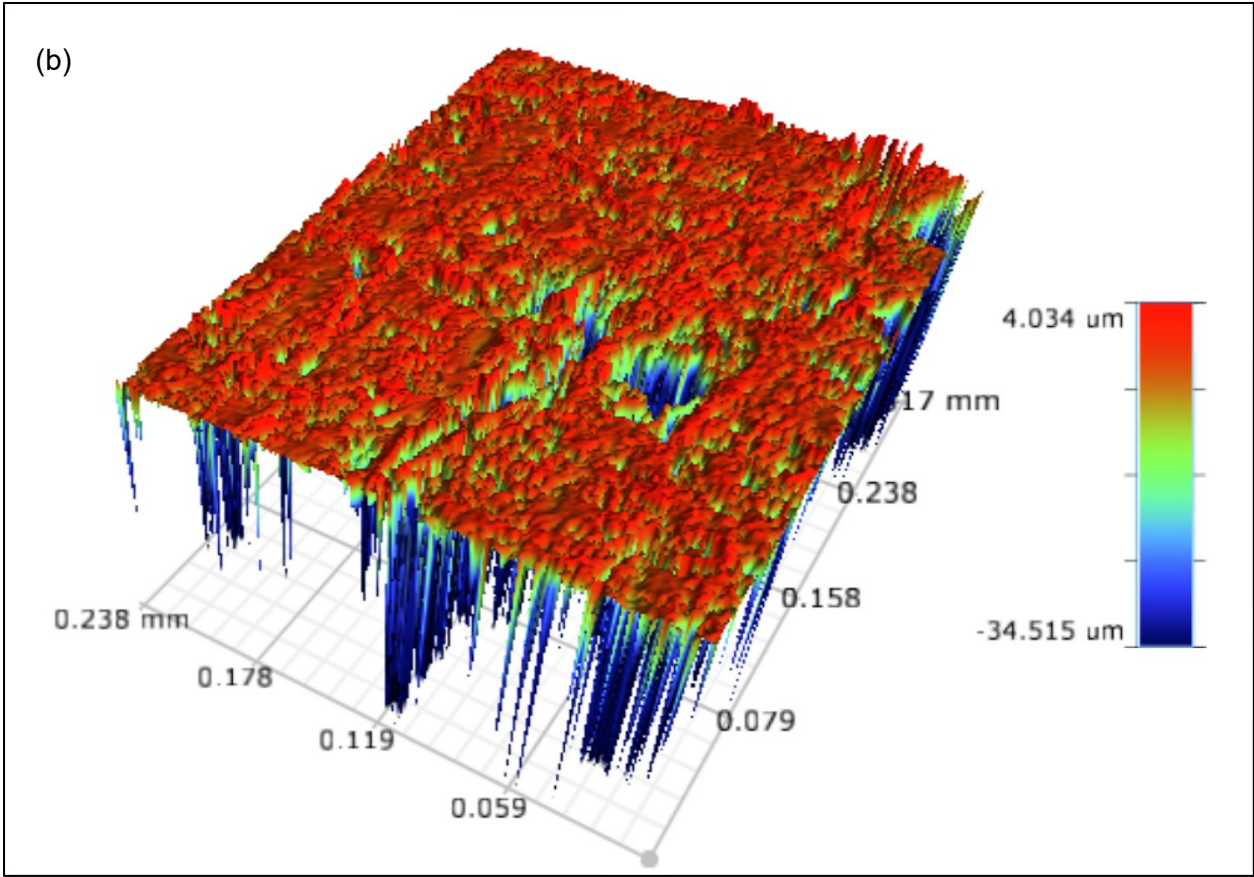
216 The influence of different sol-gel coatings on the surface roughness of hemp shiv can be seen in
217 Figure 5. The 3D surface roughness profile showed that the sol A-5 coating on the hemp shiv
218 lowered the surface roughness providing a smoother surface as seen in Figure 5b. The non-
219 uniform coating was also cracked, which in turn can facilitate water penetration into the hemp
220 shiv. On the other hand, sol A-7 (containing lower HDTMS loading) enhanced the surface

221 roughness of hemp shiv. Overall ethanol diluted sol-gel coatings had enhanced the surface
222 roughness of hemp shiv. Sol B-5 had the highest mean surface roughness as seen in Figure 5c.

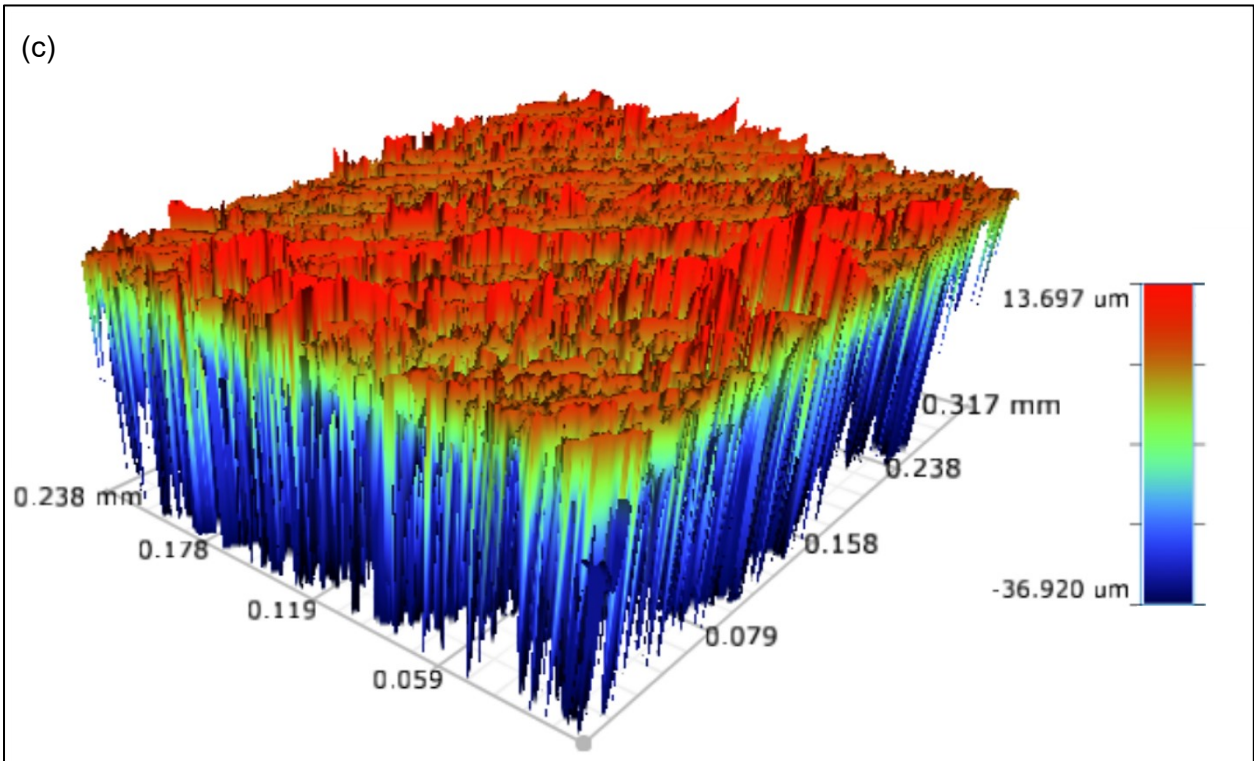
223
224



225



226
227



228

229 *Figure 5. Surface roughness of (a) uncoated, (b) sol A-5 and (c) sol B-5 coated hemp shiv surface.*

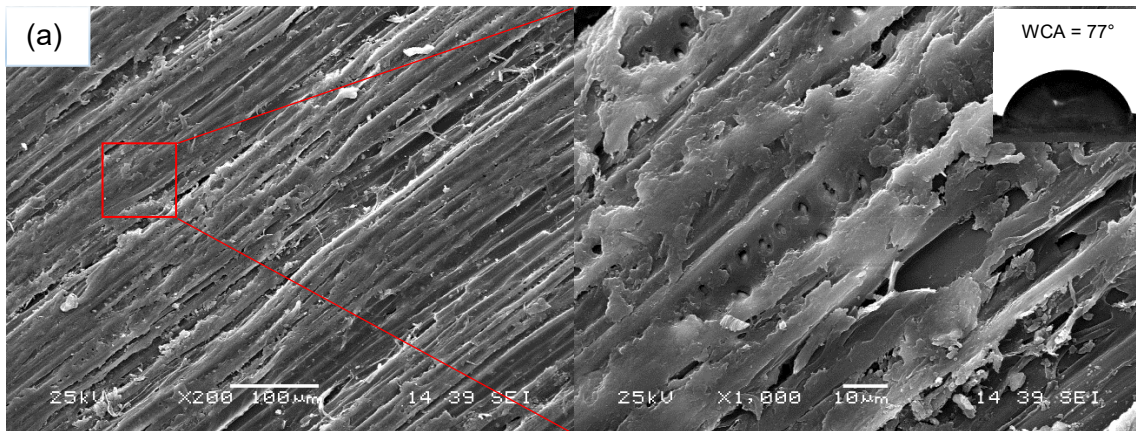
230

231 **3.3 Surface Morphology**

232 Roughness parameters alone cannot describe the surface morphology and therefore microscopy
233 analysis is beneficial to improve surface evaluations. The morphology of the uncoated and sol-
234 gel coated surfaces was studied by scanning electron microscopy (SEM). Figure 6 shows the
235 micrographs of hemp shiv surface before and after modification with different sol-gel coatings. Sol
236 A-5 and sol B-7 (Figures 6b and 6e) formed a thick coating layer and changed the morphology of
237 the shiv surface. This resulted in coating with major cracks which could be a result of shrinkage
238 after drying the treated sample (sol-gel coated hemp shiv). On the other hand, sol A-7 and sol B-
239 5 (Figures 6c and 6d) showed uniformly coated surfaces without significantly altering the
240 morphology of the hemp shiv.

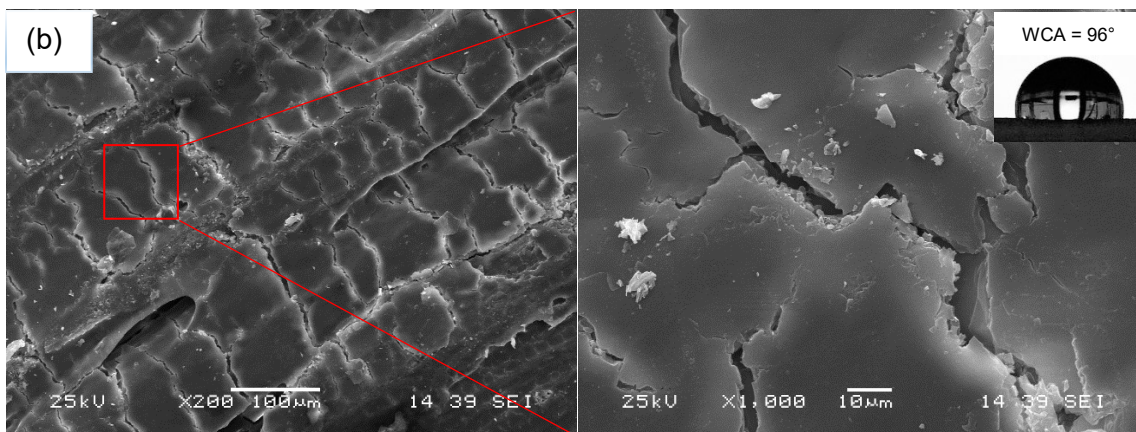
241

242



243

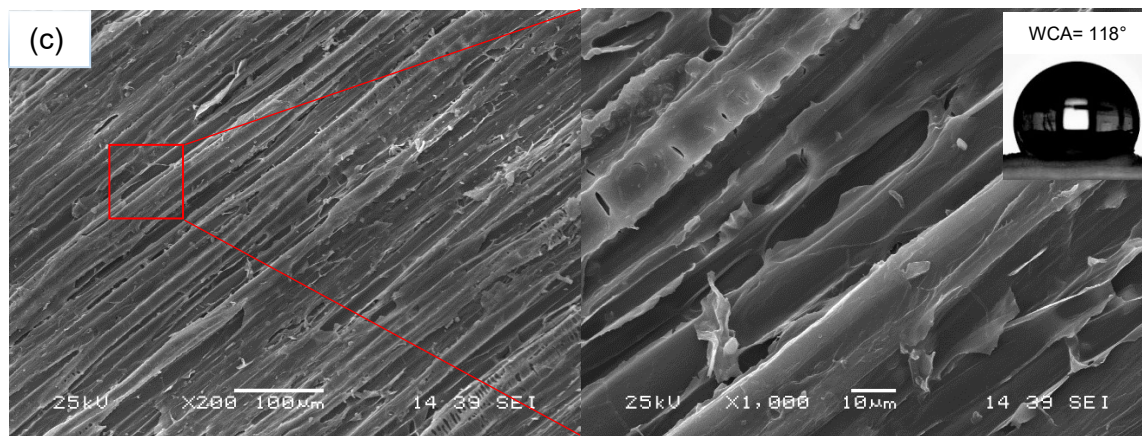
244



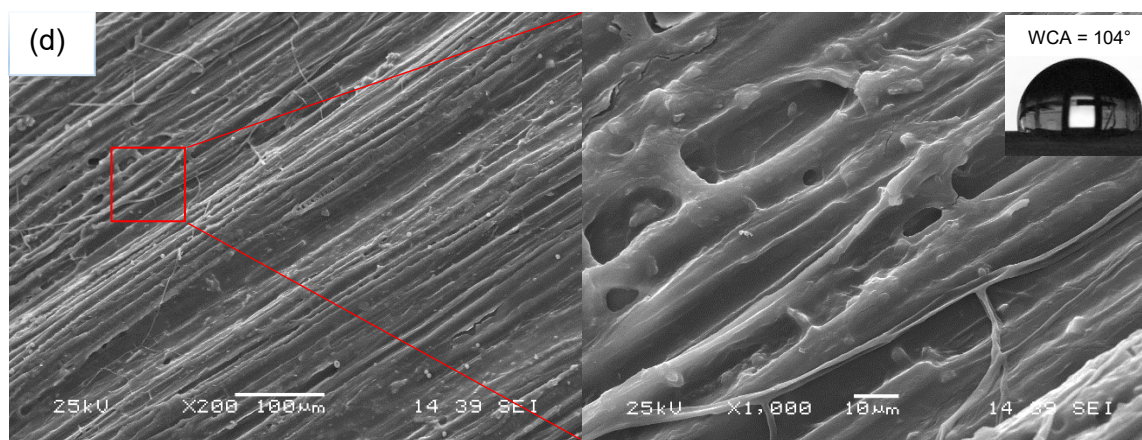
245

246

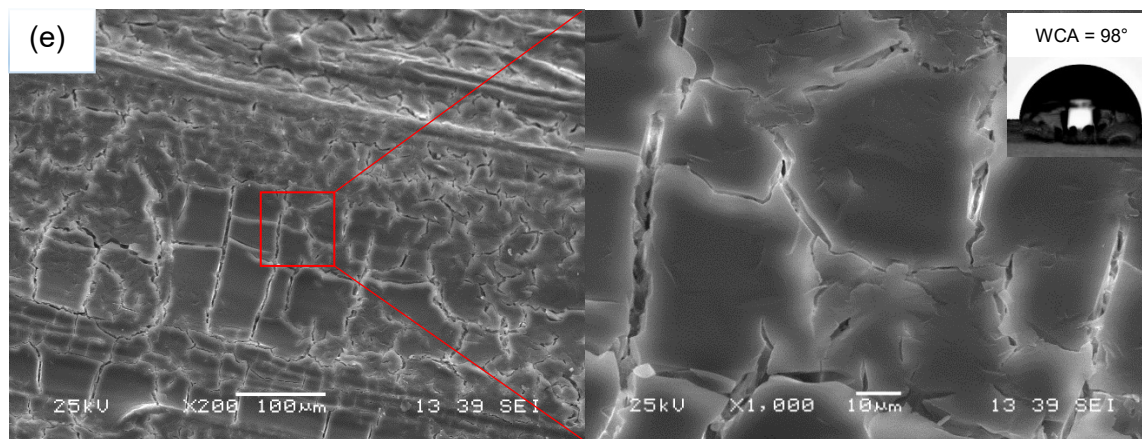
247
248

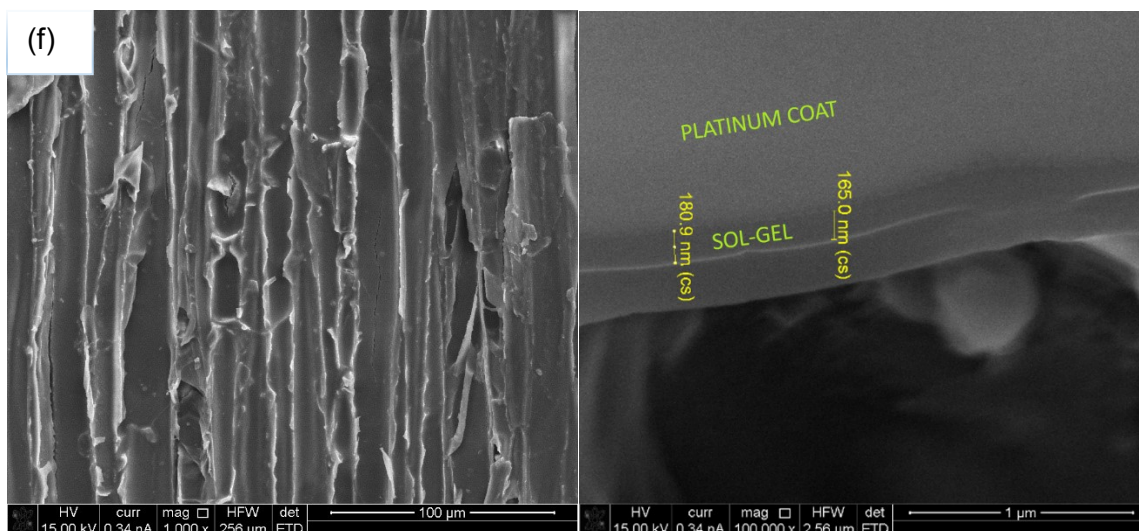


249
250



251
252





253
 254 *Figure 6. Surface morphology and WCA of (a) uncoated, (b) sol A-5, (c) sol A-7, (d) sol B-5 (e) sol B-7 coated hemp*
 255 *shiv surface and (f) thickness of sol-gel coating.*

256
 257 *Conventional SEM techniques proved unsuccessful in determining the coating thickness, but SEM-FIB*
 258 *(Focused Ion Beam) imaging of an early iteration of the formulation (Figure 6f) measured a thickness in*
 259 *the range 160-180nm. It is expected that the current formulations (sol A-7 and sol B-5) would have a*
 260 *similar thickness.*

261
 262 **3.4 Chemical Composition**

263 The surface chemical composition was determined by X-ray photoelectron spectroscopy. A low-
 264 resolution survey scan determined the atomic percentage of various elements present at the
 265 sample surface (Figure 7). The relative elemental composition of the uncoated and sol-gel coated
 266 hemp shiv surface is listed in Table 2.

267
 268 *Table 2. Relative amount of atoms at sample surface determined by low-resolution XPS scan.*

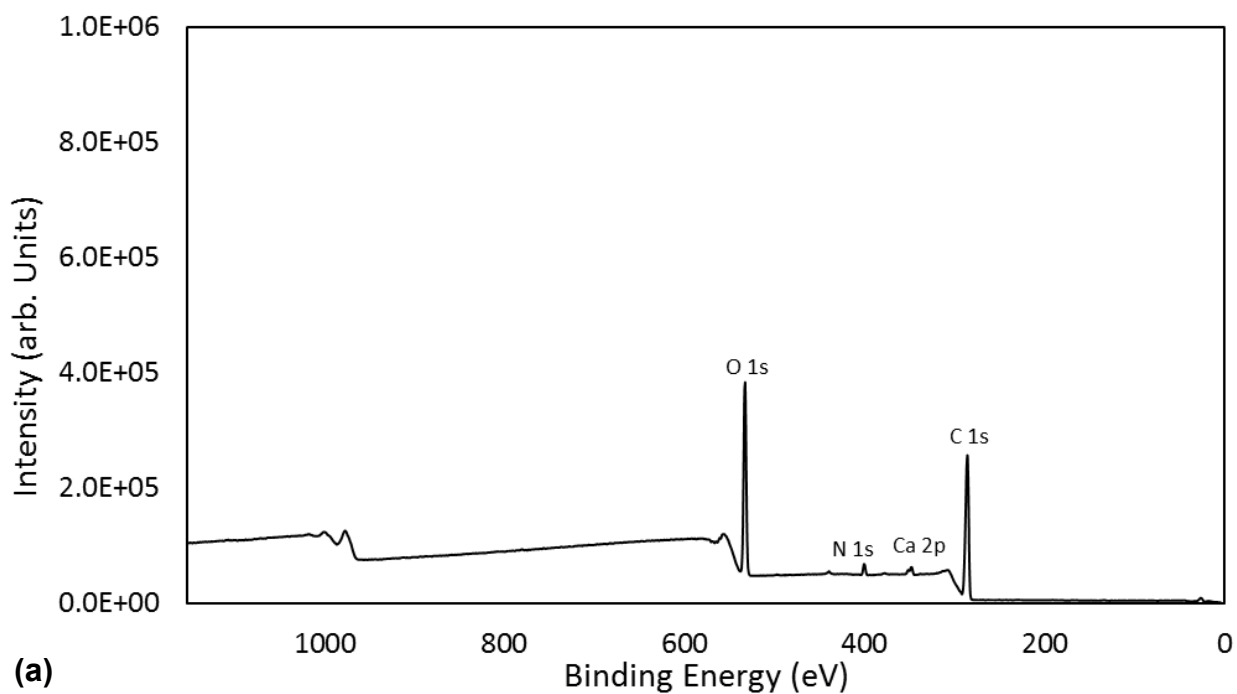
Element	Relative Conc. (atomic %)	
	Uncoated Hemp shiv	Sol A-7 Coated Hemp Shiv
C	69.61	28.33
O	27.06	53.57
N	2.06	-
Ca	0.64	-

P	0.14	-
K	0.30	-
S	0.09	-
Na	0.04	-
Cl	0.04	-
Co	0.03	-
Si	-	18.10

269

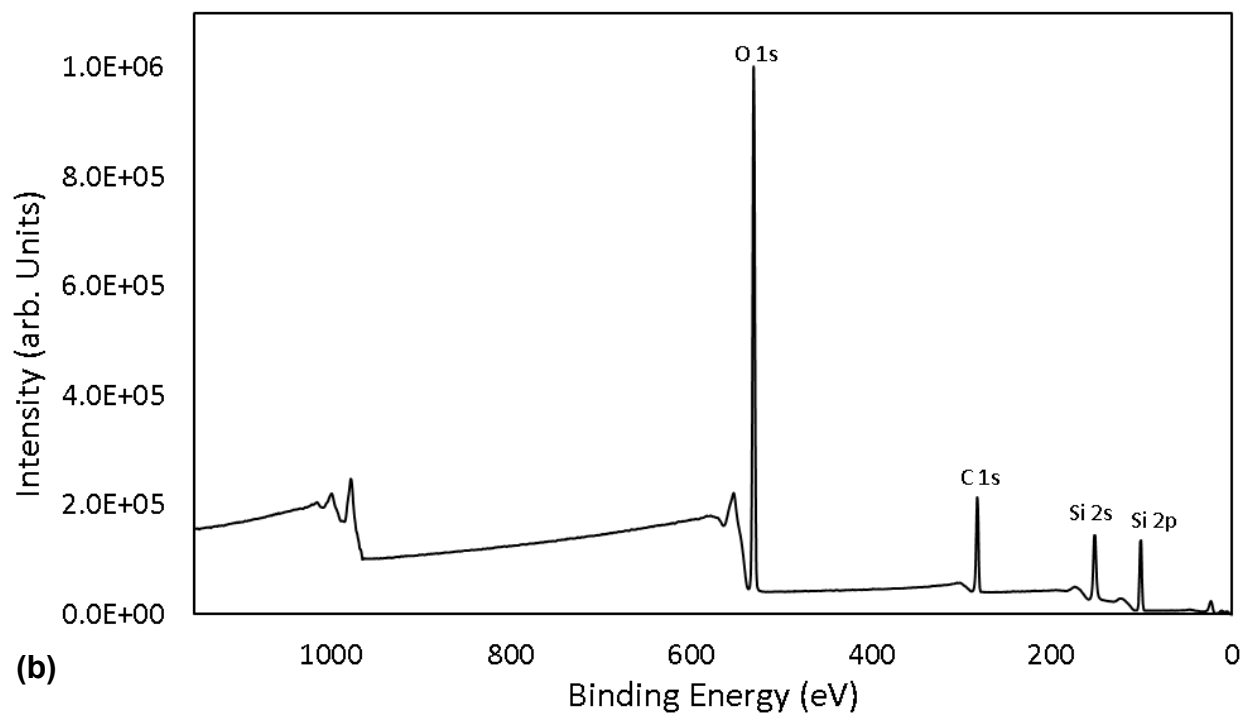
270 The main elements detected for uncoated hemp shiv were carbon and oxygen. Small amounts of
 271 other elements were present either possibly arising from the epidermal cell wall or from
 272 contamination during sample preparation. The sol-gel coated hemp shiv additionally showed high
 273 content of silicon arising from the silica based membrane on the surface (Figure 7b).

274



275

276



277
 278 *Figure 7. XPS survey scan for (a) uncoated hemp shiv, (b) sol A-7 coated hemp shiv.*

279
 280 A high-resolution scan was performed on the C1s region for the uncoated and sol-gel coated
 281 hemp shiv samples to determine the type of oxygen-carbon bonds present. The chemical bond
 282 analysis of carbon was performed by curve-fitting the C1s peak and deconvoluting it into four sub
 283 peaks corresponding to unoxidized carbon C1, and various oxidized carbons C2, C3 and C4. A
 284 ratio between oxidized carbon (C_{ox}) and unoxidized carbon (C_{unox}) was calculated by the equation
 285 [25]:

286
 287
$$C_{ox/unox} = \frac{C_{ox}}{C_{unox}} = \frac{C2+C3+C4}{C1} \quad \text{Equation 1}$$

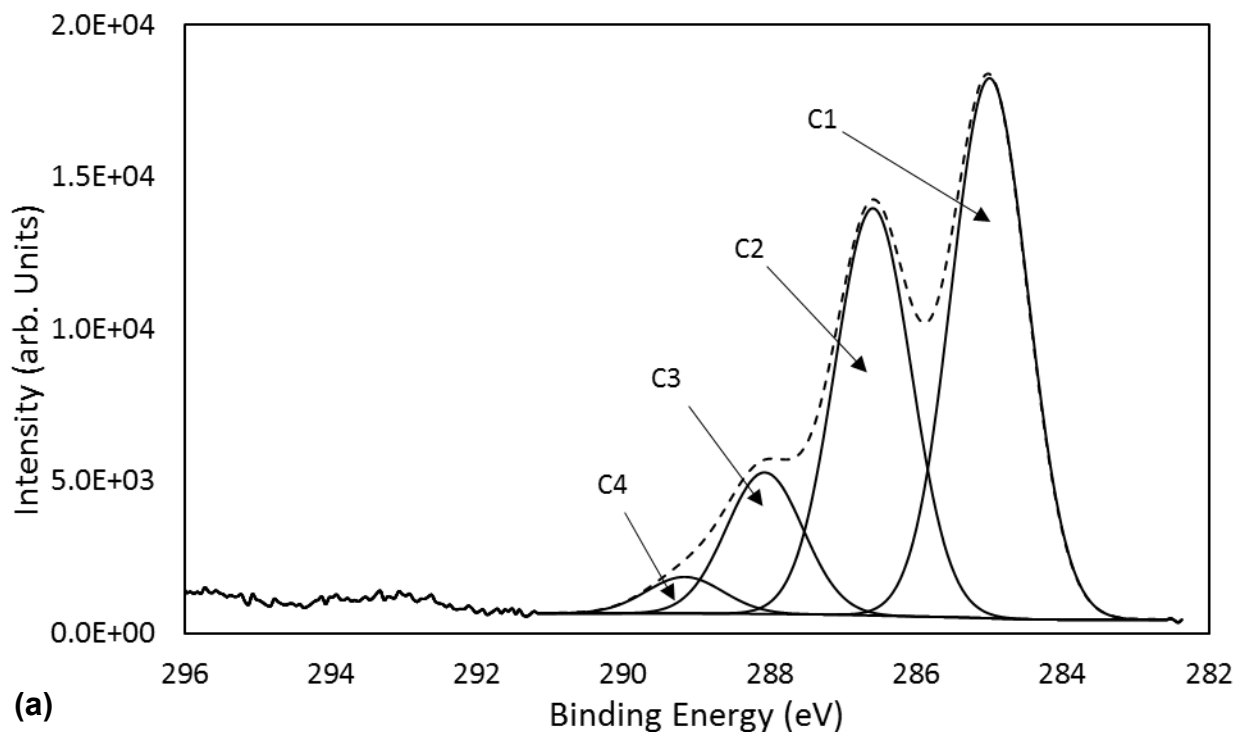
288
 289 The binding energy, corresponding bond type and their relative percentage are listed in Table 3.
 290 The ratio of $C_{ox/unox}$ has dropped significantly for sol-gel coated hemp shiv indicating that the
 291 carbon oxygen bonds have decreased on the surface of the samples.

292

293 *Table 3. Deconvoluted peak parameters and relative amount of different carbon-to-oxygen bonds at sample surface*
 294 *determined by high-resolution XPS.*

Carbon Group	Peak parameters		Relative amount (% area)	
	Binding Energy (eV)	Bond	Uncoated	Sol A-7 Coated
C1	285.0	C-C or C-H	48.01	91.09
C2	286.6/286.8	C-OH	36.18	8.91
C3	288.0	O-C-O or C=O	12.56	0.00
C4	289.2	O-C=O	3.24	0.00
C _{ox/unox}	-	-	1.08	0.09

295
 296 The C1s high resolution spectra with the deconvoluted peaks for uncoated and sol-gel coated
 297 surfaces are represented in Figure 8. The C1 peak represents carbon-carbon or carbon-hydrogen
 298 bonds whereas C2, C3, and C4 peaks possess carbon-oxygen bonds.



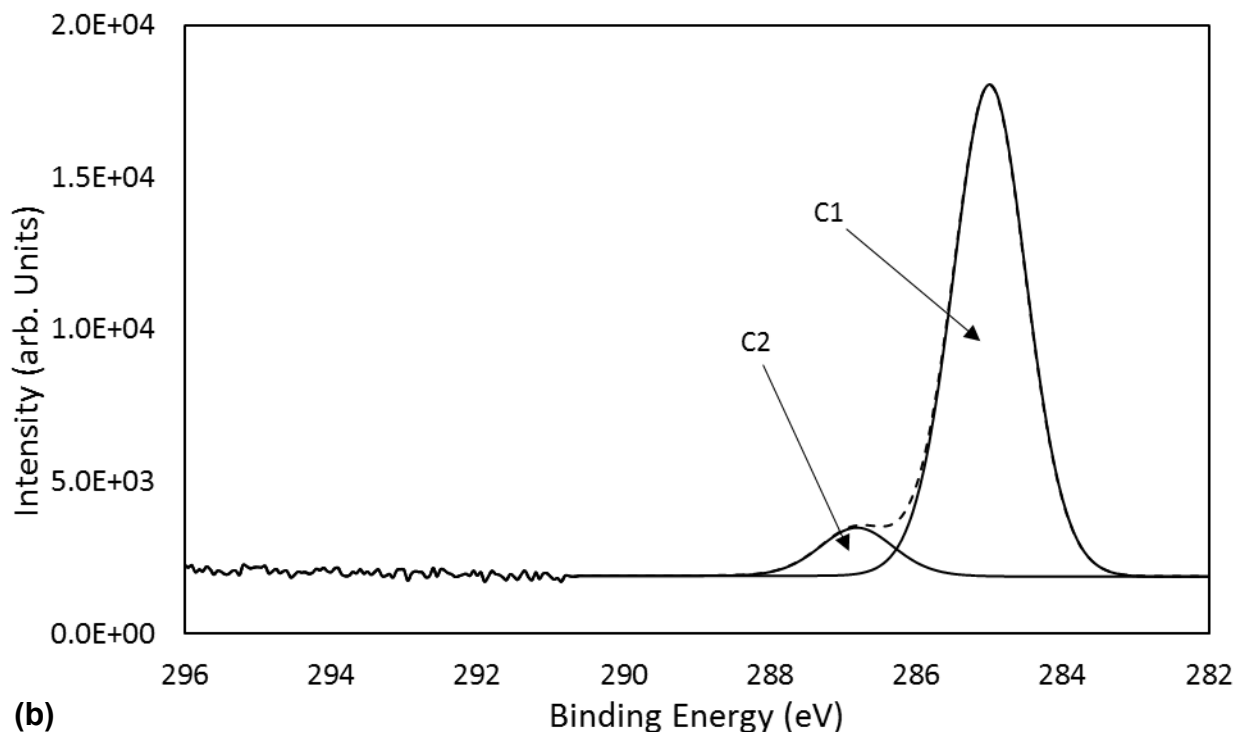


Figure 8. XPS scan of C_{1s} region for (a) uncoated hemp shiv, (b) sol A-7 coated hemp shiv.

4. Discussion

The sol-gel coatings were functionalised using HDTMS as the hydrophobic additive during the sol-gel synthesis. The co-precursor method of sol-gel synthesis was followed based on the simplicity of the process. In the sol-gel process, TEOS is hydrolysed and condensed to form a SiO_2 network which is covalently bonded to cell wall through the hydroxyl sites of cellulose present in the hemp shiv. On addition of hydrophobic agent as a co-precursor during the sol-gel processing, the hydroxyl groups on the silica clusters are replaced by the $-Si-C_{16}$ groups through oxygen bonds as illustrated in Figure 9. The hydrophobicity of the sol-gel coatings is due to the attachment of these long alkyl chains on the silica network thereby providing water resistance to the hemp shiv surface.

317

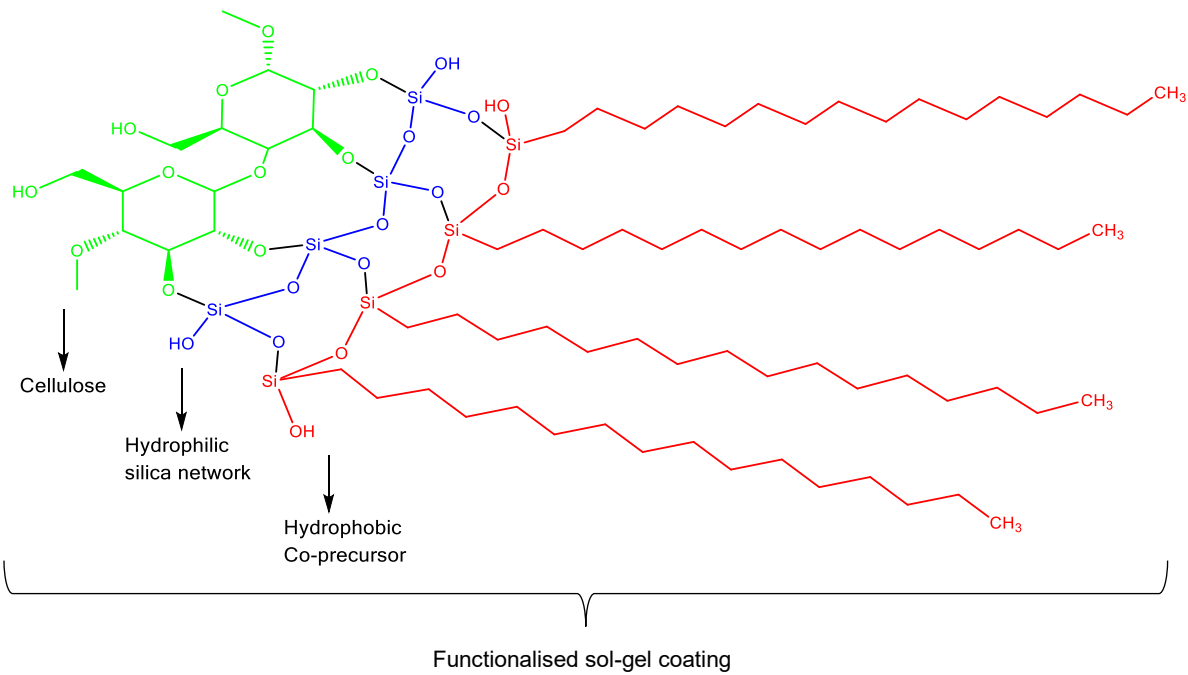


Figure 9 Schematic illustration of sol-gel deposition on glucose units of cellulose.

Overall, the acid catalysed sol-gel coatings enhance the water repellence of hemp shiv making the surface hydrophobic ($WCA > 90^\circ$). The wettability of the surface is controlled by the surface chemical composition as well as by the morphology of the microstructure. Surfaces with a similar chemical composition may have different wettability behaviour due to the surface topology [26]. In this study, the surface of hemp shiv underwent microstructural changes via deposition of an organo-functionalised silica coating.

Ethanol diluted sol series enhanced the surface roughness of the hemp shiv. At higher HDTMS loading, undiluted coatings (sol A-1 and sol A-5) lowered the surface roughness of the shiv which could explain the reason for lower contact angles compared to diluted coatings. Sol A-1 and sol A-5 have HDTMS molecules that are not fully hydrolysed and being deposited onto the membrane as a flat thick film as seen in Figure 6b. The reduced surface roughness can be attributed to the extra HDTMS molecules on the coated surface [27]. Therefore, sol-gel coatings chemically modified the surface of hemp shiv which overall improved the hydrophobicity of the material. The high water repellence can be attributed to the long alkyl chains of HDTMS that provide high hydrophobicity.

338

339 ~~Interestingly, the optimal HDTMS loading was observed when hemp shiv samples were coated~~
340 ~~with sol A-7 (1% HDTMS loading). The hemp shiv modified with sol A-7 delivered the highest~~
341 ~~contact angle, up to 118°. This can be related to the crack-free surface and the enhanced surface~~
342 ~~roughness of coated hemp shiv.~~

343

344 Since an organic-inorganic hybrid coating was used, the ratio of TEOS: HDTMS was critical to
345 control the roughness of the coatings resulting in variable water repellent properties of the coated
346 hemp shiv. Most of the coatings enhanced the surface roughness except sol A-1 and sol A-5.
347 These coatings had smooth surfaces with cracks which could explain the lower contact angles
348 even though it had the highest loading of hydrophobic agent. ~~It was observed that the TEOS:~~
349 ~~HDTMS molar ratio in the coating formulations affected the hydrophobicity of the coated~~
350 ~~hemp shiv. From Figure 3 it can be seen that varying the concentration of HDTMS in the~~
351 ~~formulations affects the water contact angle. When TEOS: HDTMS was 1: 0.01 corresponding~~
352 ~~to 0.5 wt% HDTMS, the contact angle was below 100° which suggests the concentration of~~
353 ~~the hydrophobic agent was too low to provide sufficient level of hydrophobicity . The best~~
354 ~~results were obtained with TEOS: HDTMS ratio 1: 0.02 (1 wt% HDTMS)with contact angles up~~
355 ~~to 118°. However, when the TEOS: HDTMS ratio was increased to 1: 0.06 (4 wt% HDTMS), the~~
356 ~~hydrophobicity was decreased for the undiluted sol coatings. These results can be explained~~
357 ~~by the combined effect of surface roughness and energy. TEOS is hydrophilic whereas HDTMS~~
358 ~~is hydrophobic and changing their molar ratio can affect the surface roughness and energy~~
359 ~~of the coated material. Increasing the HDTMS concentration would reduce the surface energy.~~
360 ~~However the surface roughness can be reduced if the HDTMS concentration is high enough~~
361 ~~as the extra silane fills the inter-particle gap. Similar results have been reported in different~~
362 ~~coating systems [27,28]. Although sol B-7 coating enhanced the surface roughness, it had~~
363 ~~developed cracks which lowered the water contact angle to 98°. The presence of surface cracks~~
364 ~~arising as a result of shrinkage after drying the coated shiv is a significant factor to be considered~~
365 ~~when hydrophobic properties are concerned. The hydrophobicity of modified hemp shiv can be~~
366 ~~compromised as the water molecules can penetrate through the cracked coating wetting the bulk~~
367 ~~of the material over time. Therefore, sol-gel coatings chemically modified the surface of hemp~~

368 shiv which overall improved the hydrophobicity of the material. The high water repellence can be
369 attributed to the long alkyl chains of HDTMS that provide high hydrophobicity.

370
371 The chemical composition of hemp shiv is mainly composed of cellulose, hemicellulose and lignin,
372 which altogether contain a large percentage of oxidized carbon in their structure. Hydroxyl groups
373 are known to contribute towards majority of the carbon-oxygen bonds in bio-based materials [29].
374 The XPS data confirmed that the sol-gel deposition on hemp shiv significantly altered the surface
375 chemistry. The surface carbon content of the coated hemp shiv decreased by 41.28% (from 69.61
376 to 28.33%). On the other hand, the oxygen content increased by 26.51% (from 27.06 to 53.57%).
377 This change in C/O ratio and increase in surface oxygen concentration can be attributed to O-
378 CH₃ bonds present in the polysiloxane coating on the surface of the sol-gel coated hemp shiv.
379 Moreover, the decrease in the surface carbon concentration of the sol-gel coated shiv can be
380 attributed to the masking effect of the polysiloxane coating which reduces the detectability of
381 surface cellulose and hemicellulose.

382
383 The C1s high resolution XPS spectra indicate that the surface has been modified by the silica
384 based coating that led to disappearance of C3 and C4 components of the C1s peaks. A shift in
385 the binding energy of C2 component (from 286.6 to 286.8 eV) was observed along with the
386 decrease in the intensity of the C2 component for the sol-gel coated sample. This shift indicates
387 the presence of a carbon atom linked to an oxygen and silicon atom (O-C-Si or C-O-Si) [18]. It
388 has also been shown [16,30–32] that curing above room temperature drives the dehydration
389 reaction at the adsorption sites between hydroxyl groups of the cellulose and the silanols forming
390 –Si-O-C- bonds. These bonds are formed by the linkage between polysilanol network with the
391 cellulose hydroxyl groups via polycondensation as illustrated in Figure 9. The increase in the
392 intensity of C1 component for sol-gel coated sample from 48.01% to 91.09% indicates the
393 presence of C-H and C-C bonds from the HDTMS hydrocarbon chain.

394

395 **5. Conclusion**

396 A simple one step dip-coating process was successfully applied to form a hydrophobic surface
397 onto an extremely hydrophilic bio-based aggregate construction material. The hydrophobic
398 properties were achieved through a combination of topological alteration and chemical
399 modification of the hemp shiv by the modified silica based sol-gel coatings.

400

401 The treated material (hemp shiv coated with silica based membrane) delivered the following
402 properties when compared to the untreated hemp shiv:

- 403 • Delivered water repellence by maintaining stable water contact angles over 60 seconds.
- 404 • Controlled surface wettability through microstructure modification.
- 405 • Uniform and crack-free coated surface.
- 406 • Enhanced surface roughness providing water contact angles up to 118°.

407

408 It can be concluded that water based sol-gel coatings with low HDTMS precursor loading (sol A-
409 7) would be of interest to the bio-based building industry due to its hygroscopic properties, long
410 shelf life, reduced cost and lower environmental impact.

411

412 **Acknowledgments**

413 This study was supported by the Canadian Queen Elizabeth II Diamond Jubilee Scholarship and
414 the ISOBIO project funded by the Horizon 2020 programme [grant number 636835 – ISOBIO –
415 H2020-EeB-2014-2015]. The authors would also like to acknowledge the EPSRC Centre for
416 Decarbonisation of the Built Environment (dCarb) [grant number EP/L016869/1] and the NSERC
417 project (grant number IRCPJ 461745-12). The ISOBIO project aims to develop and bring new bio-
418 based insulation panels and renders into the mainstream for the purpose of creating more energy
419 efficient buildings. The contents of this publication are the sole responsibility of the authors and
420 can in no way be taken to reflect the views of the European Union.

421

422 **References**

- 423 [1] J. Genzer, K. Efimenko, Recent developments in superhydrophobic surfaces and their
424 relevance to marine fouling: a review., *Biofouling*. 22 (2006) 339–360.
425 doi:10.1080/08927010600980223.
- 426 [2] A. Nakajima, K. Hashimoto, T. Watanabe, Recent studies on super-hydrophobic films, in:
427 *Monatshefte Fur Chemie*, 2001: pp. 31–41. doi:10.1007/s007060170142.
- 428 [3] S. Benfratello, C. Capitano, G. Peri, G. Rizzo, G. Scaccianoce, G. Sorrentino, Thermal and
429 structural properties of a hemp-lime biocomposite, *Constr. Build. Mater.* 48 (2013) 745–
430 754. doi:10.1016/j.conbuildmat.2013.07.096.
- 431 [4] A.D. Tran Le, C. Maalouf, T.H. Mai, E. Wurtz, F. Collet, Transient hygrothermal behaviour
432 of a hemp concrete building envelope, *Energy Build.* 42 (2010) 1797–1806.

- 433 doi:10.1016/j.enbuild.2010.05.016.
- 434 [5] L. Arnaud, E. Gourlay, Experimental study of parameters influencing mechanical properties
435 of hemp concretes, *Constr. Build. Mater.* 28 (2012) 50–56.
436 doi:10.1016/j.conbuildmat.2011.07.052.
- 437 [6] M. Theis, B. Grohe, Biodegradable lightweight construction boards based on
438 tannin/hexamine bonded hemp shaves, *Holz Als Roh - Und Werkst.* 60 (2002) 291–296.
439 doi:10.1007/s00107-002-0306-0.
- 440 [7] H. Kyma, M. Hautala, R. Kuisma, A. Pasila, Capillarity of flax / linseed (*Linum usitatissimum*
441 L.) and fibre hemp (*Cannabis sativa* L.) straw fractions, 14 (2001) 41–50.
- 442 [8] J. Gassan, V.S. Gutowski, A.K. Bledzki, About the surface characteristics of natural fibres,
443 *Surf. Eng.* 283 (2000) 132–139. doi:10.1002/1439-2054(20001101)283:1<132::AID-
444 MAME132>3.0.CO;2-B.
- 445 [9] S. Marceau, P. Glé, M. Guéguen-Minerbe, E. Gourlay, S. Moscardelli, I. Nour, S. Amziane,
446 Influence of accelerated aging on the properties of hemp concretes, *Constr. Build. Mater.*
447 139 (2017) 524–530. doi:10.1016/j.conbuildmat.2016.11.129.
- 448 [10] L. Kidalova, N. Stevulova, E. Terpakova, Influence of water absorption on the selected
449 properties of hemp hurds composites, *Pollack Period.* (2015).
450 doi:10.1556/Pollack.10.2015.1.12.
- 451 [11] M.R. Vignon, D. Dupeyre, Steam explosion of woody hemp ch nevotte, 17 (1995) 395–
452 404.
- 453 [12] M.M. Kabir, H. Wang, K.T. Lau, F. Cardona, Chemical treatments on plant-based natural
454 fibre reinforced polymer composites: An overview, *Compos. Part B Eng.* 43 (2012) 2883–
455 2892. doi:10.1016/j.compositesb.2012.04.053.
- 456 [13] S. Donath, H. Militz, C. Mai, Wood modification with alkoxysilanes, *Wood Sci. Technol.* 38
457 (2004) 555–566. doi:10.1007/s00226-004-0257-1.
- 458 [14] E. Cabane, T. Keplinger, V. Merk, P. Hass, I. Burgert, Renewable and functional wood
459 materials by grafting polymerization within cell walls, *ChemSusChem.* 7 (2014) 1020–1025.
460 doi:10.1002/cssc.201301107.
- 461 [15] J. Song, O.J. Rojas, Approaching super-hydrophobicity from cellulosic materials: A
462 Review, *Pap. Chem.* 28 (2013) 216–238. doi:10.3183/NPPRJ-2013-28-02-p216-238.
- 463 [16] A. Valadez-Gonzalez, J.M. Cervantes-Uc, R. Olayo, P.J. Herrera-Franco, Effect of fiber
464 surface treatment on the fiber-matrix bond strength of natural fiber reinforced composites,
465 *Compos. Part B Eng.* 30 (1999) 309–320. doi:10.1016/S1359-8368(98)00054-7.
- 466 [17] C. Brinker, G. Scherer, *Sol-Gel Science: The Physics and Chemistry of Sol-Gel*

- 467 Processing, *Adv. Mater.* 3 (1990) 912. doi:10.1186/1471-2105-8-444.
- 468 [18] M.A. Tshabalala, P. Kingshott, M.R. Vanlandingham, D. Plackett, *Surface Chemistry and*
469 *Moisture Sorption Properties of Wood Coated with Multifunctional Alkoxysilanes by Sol-*
470 *Gel Process*, (2002).
- 471 [19] B. Tomšič, B. Simončič, B. Orel, L. Černe, P.F. Tavčer, M. Zorko, I. Jerman, A. Vilčnik, J.
472 Kovač, *Sol-gel coating of cellulose fibres with antimicrobial and repellent properties*, *J.*
473 *Sol-Gel Sci. Technol.* 47 (2008) 44–57. doi:10.1007/s10971-008-1732-1.
- 474 [20] L. Xu, W. Zhuang, B. Xu, Z. Cai, *Superhydrophobic cotton fabrics prepared by one-step*
475 *water-based sol-gel coating*, *J. Text. Inst.* 103 (2012) 311–319.
476 doi:10.1080/00405000.2011.569238.
- 477 [21] S. Sankaraiah, J.M. Lee, J.H. Kim, S.W. Choi, *Preparation and characterization of surface-*
478 *functionalized polysilsesquioxane hard spheres in aqueous medium*, *Macromolecules.* 41
479 (2008) 6195–6204. doi:10.1021/ma8003345.
- 480 [22] Y. Fujiwara, Y. Fujii, Y. Sawada, S. Okumura, *Assessment of wood surface roughness:*
481 *Comparison of tactile roughness and three-dimensional parameters derived using a robust*
482 *Gaussian regression filter*, *J. Wood Sci.* 50 (2004) 35–40. doi:10.1007/s10086-003-0529-
483 7.
- 484 [23] L. Gurau, H. Mansfield-Williams, M. Irle, *Filtering the roughness of a sanded wood surface*,
485 *Holz Als Roh - Und Werkst.* 64 (2006) 363–371. doi:10.1007/s00107-005-0089-1.
- 486 [24] B. Ugulino, R.E. Hernández, *Assessment of surface properties and solvent-borne coating*
487 *performance of red oak wood produced by peripheral planing*, *Eur. J. Wood Wood Prod.*
488 (2016) 1–13. doi:10.1007/s00107-016-1090-6.
- 489 [25] N.M. Stark, L.M. Matuana, *Surface chemistry changes of weathered HDPE/wood-flour*
490 *composites studied by XPS and FTIR spectroscopy*, *Polym. Degrad. Stab.* 86 (2004) 1–9.
491 doi:10.1016/j.polymdegradstab.2003.11.002.
- 492 [26] Q.F. Xu, J.N. Wang, K.D. Sanderson, *Organic-inorganic composite nanocoatings with*
493 *superhydrophobicity, good transparency, and thermal stability*, *ACS Nano.* 4 (2010) 2201–
494 2209. doi:10.1021/nn901581j.
- 495 [27] H. Wang, H. Zhou, S. Liu, H. Shao, S. Fu, G.C. Rutledge, T. Lin, *Durable, self-healing,*
496 *superhydrophobic fabrics from fluorine-free, waterborne, polydopamine/alkyl silane*
497 *coatings*, *RSC Adv.* 7 (2017) 33986–33993. doi:10.1039/C7RA04863G.
- 498 [28] C. Zeng, H. Wang, H. Zhou, T. Lin, *Self-cleaning, superhydrophobic cotton fabrics with*
499 *excellent washing durability, solvent resistance and chemical stability prepared from an*
500 *SU-8 derived surface coating*, *RSC Adv.* 5 (2015) 61044–61050.

- 501 doi:10.1039/C5RA08040A.
- 502 [29] N.M. Stark, L.M. Matuana, Ultraviolet weathering of photostabilized wood-flour-filled high-
503 density polyethylene composites, *J. Appl. Polym. Sci.* 90 (2003) 2609–2617.
504 doi:10.1002/app.12886.
- 505 [30] Y. Xie, C.A.S. Hill, Z. Xiao, H. Militz, C. Mai, Silane coupling agents used for natural
506 fiber/polymer composites: A review, *Compos. Part A Appl. Sci. Manuf.* 41 (2010) 806–819.
507 doi:10.1016/j.compositesa.2010.03.005.
- 508 [31] M. Castellano, A. Gandini, P. Fabbri, M.N. Belgacem, Modification of cellulose fibres with
509 organosilanes: Under what conditions does coupling occur?, *J. Colloid Interface Sci.* 273
510 (2004) 505–511. doi:10.1016/j.jcis.2003.09.044.
- 511 [32] M. Abdelmouleh, S. Boufi, M.N. Belgacem, A. Dufresne, Short natural-fibre reinforced
512 polyethylene and natural rubber composites: Effect of silane coupling agents and fibres
513 loading, *Compos. Sci. Technol.* 67 (2007) 1627–1639.
514 doi:10.1016/j.compscitech.2006.07.003.
- 515